Direct Electrochemistry of Porcine Purple Acid Phosphatase (Uteroferrin)†

Paul V. Bernhardt,* Gerhard Schenk, and Gregory J. Wilson

Center for Metals in Biology, Department of Chemistry, University of Queensland, Brisbane 4072, Australia

Received May 13, 2004; Revised Manuscript Received June 15, 2004

ABSTRACT: Cyclic voltammetry of the non-heme diiron enzyme porcine purple acid phosphatase (uteroferrin, Uf) has been reported for the first time. Totally reversible one-electron oxidation responses ($Fe^{III}-Fe^{II} \rightarrow Fe^{III}-Fe^{III}$) are seen both in the absence and in the presence of weak competitive inhibitors phosphate and arsenate, and dissociation constants of these oxoanion complexes formed with uteroferrin in its oxidized state (Uf_o) have been determined. The effect of pH on the redox potentials has been investigated in the range $3 < pH < 6.5$, enabling acid dissociation constants for Uf_o and its phosphate and arsenate complexes to be calculated.

The purple acid phosphatases (PAPs)[1] (*1*, *2*) comprise a subfamily of non-heme dinuclear iron containing proteins that also include the ribonucleotide reductases, methane monooxygenases, and hemerythrins (*3*). Several types of PAPs have been isolated and studied from various plant (*4*−*7*) and animal (*8*, *9*) sources, although they appear to be even more widespread in nature (*10*). Unlike other non-heme dinuclear iron proteins, PAPs do not appear to undergo redox transformations as a part of their function. Instead, they catalyze the hydrolysis of a range of phosphate esters under acidic conditions. However, their exact physiological function remains uncertain (*11*). Recent data point to a role for mammalian PAPs in bone resorption and raise the possibility that the enzyme may be a drug design target for the treatment of osteoporosis (*12*, *13*).

Crystal structures have been reported for PAPs isolated from pig uterus, also known as uteroferrin or Uf (Figure 1) (*14*), rat bone (*15*), and red kidney bean (*16*, *17*). All PAPs bear an active site comprising a ferric ion (site A) and a divalent metal ion (site B). In mammalian enzymes, the divalent metal ion is Fe (*8*, *9*), whereas in plant PAPs it may be Zn or Mn. (*5*) Metal site A (Fe^{III}) is coordinated to terminal tyrosine, histidine, and aspartate ligands. The terminal amino acid ligands to the divalent ion comprise two histidines and an asparagine. The two metal sites are simultaneously bridged by an aspartate and a water-based ligand. Oxoanions such as phosphate are known to bind to the active site of PAPs (such as Uf; Figure 1) (*14*). EXAFS studies on phosphate free reduced ($Fe^{III}-Fe^{II}$) Uf (*18*) and its $Fe^{III}-Zn^{II}$ analogue (*19*, *20*) have suggested that water-based (aqua/hydroxo) ligands complete six-coordinate, distorted octahedral coordination spheres at both metal sites. However, direct evidence for the exact number of water-based ligands present in this active form is lacking. Red kidney bean ($Fe^{III}-Zn^{II}$) PAP is the only member of this family to have been characterized crystallographically in its oxoanion-free form (*16*, *17*), but the resolution of these structures was too low to locate any terminal or bridging water-based ligands. Recent ENDOR spectroscopic studies (*21*) have suggested that U_f in its phosphate-free reduced form bears a single terminal aqua/hydroxo ligand coordinated to the Fe^{II} ion, but the ferric site is five coordinate.

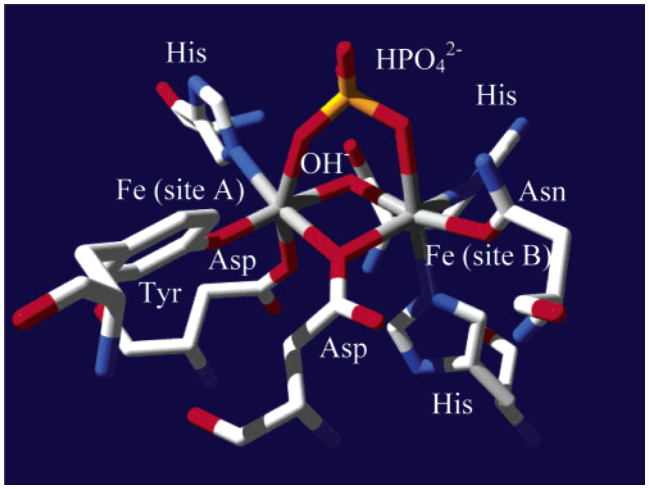

FIGURE 1: Active site of Uf in its phosphate-inhibited form (from ref *14*).

Uteroferrin is the most thoroughly studied PAP (*8*, *22*−*28*). In its reduced, catalytically active state (Uf_r), the active site comprises an antiferromagnetically coupled (*29*, *30*) mixed valent $Fe^{III}-Fe^{II}$ center. The asymmetric coordination environment of the two Fe ions in U_f (Figure 1) is also reflected in their distinct redox behavior. The ferric site is redox inert, while the ferrous ion may be oxidized to yield a catalytically inactive di-Fe^{III} form (Uf_o), which is also antiferromagnetically coupled (*22*, *29*). Uf_r undergoes pH-dependent product (phosphate) inhibition (K_i 0.8−25 mM,

† The School of Molecular and Microbial Sciences, University of Queensland is thanked for financial support of this work.

* To whom correspondence should be addressed. E-mail: P.Bernhardt@uq.edu.au. Tel.: +61 7 3365 4266. Fax: +61 7 3365 4299.

[1] Abbreviations: PAP, purple acid phosphatase; Uf, uteroferrin (Uf_o oxidized $Fe^{III}-Fe^{III}$ form; Uf_r reduced $Fe^{III}-Fe^{II}$ form); EXAFS, extended X-ray absorption fine-structure specroscopy; NHE, normal hydrogen electrode; DDAB, didodecyldimethylammonium bromide.

10.1021/bi0490338 CCC: $27.50
Published on Web 07/24/2004

pH 3−6) (*23*). The labile ferrous ion in Uf_r has been replaced by other divalent metal ions such as Mn, Co, Ni, Cu, and Zn (*20*, *28*, *31*, *32*), with retention of phosphatase activity. The ferric ion has been replaced by analogues such as Al^{III} and Ga^{III} to generate catalytically active enzymes, whereas the In^{III} analogue was inactive (*33*).

Despite the intimate coupling between oxidation state and enzymatic activity in PAPs, the electrochemical properties of PAPs have received very little attention. Wang et al. reported (*34*) the redox potentials of Uf as a function of pH and also in the presence of selected oxoanions using microcoulometry. This technique, a hybrid form of voltammetry and potentiometry, relies on the use of redox mediators to poise the solution potential and to relay electrons between the working electrode and the protein active site. No direct (unmediated) electrochemical studies of a PAP have been reported.

Unmediated protein voltammetry is becoming an increasingly popular technique for the electrochemical investigation of redox active proteins (*35*). Typically, the protein is immobilized within a thin film coated onto the working electrode surface where heterogeneous electron transfer may take place without diffusion control. Moreover, voltammetry is a time-dependent experiment and enables the investigation of chemical reactions (including their rates) coupled to electron transfer. It is this technique that we have employed in this work to investigate the direct electrochemistry of Uf. In addition, we have examined the influences of the redox-inactive inhibitors phosphate and arsenate on the electrochemistry of Uf.

EXPERIMENTAL PROCEDURES

Uteroferrin was prepared as previously described (*36*). Electrochemical measurements were carried out with a BAS 100B/W electrochemical analyzer and a BAS C3 cell stand. An edge plane pyrolytic graphite-working electrode, cleaned as described previously (*37*), a Pt wire counter electrode, and an Ag/AgCl reference electrode were employed for all experiments. All potentials are cited versus the normal hydrogen electrode (NHE) using a correction of +196 mV for the potential of the reference electrode. The working electrode protein film was prepared by first mixing 5 μL of a 200 μM solution of protein with 5 μL of a 2 mM solution of the surfactant dimethyldidodecylammonium bromide (DDAB). The resulting solution was added to the inverted working electrode and dried overnight in a refrigerator.

All electrochemical measurements were made at 25 °C in 400 μL of a mixed buffer solution comprising bis-tris propane (20 mM) and 2-amino-2-methylpropan-1-ol (20 mM) titrated with the appropriate amount of acetic acid or NaOH to give a final pH within the range 3−7. The supporting electrolyte was 10 mM NaCl. The solution was purged with argon prior to inserting the working electrode, and a blanket of argon was maintained during the experiment. For experiments in the presence of inhibiting anions, enzyme electroactivity was first established, and then the appropriate salt was added directly to the electrochemical cell to give final concentrations of 100 mM KH_2PO_4 or 50 mM NaH_2AsO_4. The reported voltammograms were initiated in the anodic (oxidizing) direction (i.e., starting with the protein poised in its reduced form Uf_r), although experiments initiated in the cathodic direction gave identical results. Cyclic voltammetry scan rates were varied in the range of 20−200 mV s^{-1}, while for square wave voltammetry the step potential was 2 mV, the square wave amplitude was 8 mV, and the square wave frequency was 5 Hz. Background subtraction of cyclic voltammetry waves was done with the program UTILS (*38*).

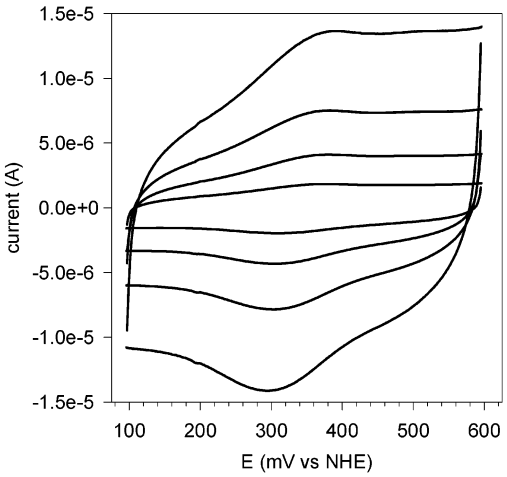

FIGURE 2: Cyclic voltammograms of Uf at pH 4.1. Curves are in order of increasing current magnitude at scan rates 20, 50, 100, and 200 mV s^{-1}.

RESULTS AND DISCUSSION

A number of enzyme electrode preparations were investigated comprising various combinations of nonredox active promoters (kanamycin, polymixin, polylysine) and also other electrode surfaces (basal plane pyrolytic graphite, gold modified with 4-mercaptopyridine), but none were as effective as the DDAB surfactant film method employing an edge plane pyrolytic graphite electrode. The electroactive protein film gave stable electrochemical responses for a period of a few hours at room temperature.

The cyclic voltammograms of Uf at pH 4.1 are shown in Figure 2 as a function of scan rate. A totally reversible one-electron couple is seen with the averaged peak potential of 344 mV versus NHE. The same voltammograms corrected for background current (Figure 3) enabled a more accurate determination of the scan rate dependence of the peak currents (Figure 3, inset). The linear dependence on scan rate is indicative of a surface confined electrochemical reaction (i.e., electron transfer is not diffusion controlled). On the basis of a single electron-transfer process, and the averaged gradients of the cathodic (-9.7×10^{-9}) and anodic peak (8.9×10^{-9}) current plots, we calculate an electroactive surface coverage of 10 pmol of protein (*39*). This is about 1% of protein used in the electrode preparation. Some protein inevitably will adsorb onto insulated parts of the electrode casing, and also some may leach from the film into the buffer and be inaccessible for electron transfer. It is also possible that multilayers of protein form within the film, but only the proteins nearest the electrode surface are accessible. Overall, the amounts of Uf that were required for reproducible voltammetry are about an order of magnitude greater than we have used in other studies of cytochrome P450s (*40*) and molybdoenzymes (*41*) immobilized within surfactant films.

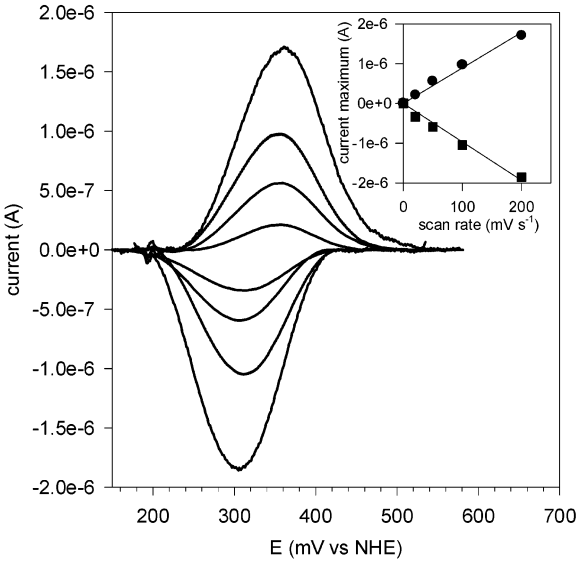

FIGURE 3: Background corrected cyclic voltammograms of Uf at pH 4.1 in order of increasing current magnitude (20, 50, 100, and 200 mV s^{-1}). Inset: linear scan rate dependence of anodic and cathodic current maxima.

The peak potentials do not change within the scan rate range of 20−200 mV s^{-1}, which reflects facile electron transfer. The peak width at half-height remains fairly constant (100−120 mV) and is consistent with that expected for a single electron-transfer reaction of an adsorbed species (91 mV at 25 °C) (*39*). Finally, the ratio of cathodic to anodic peak currents is approximately unity in all cases (ratio of gradients in the inset to Figure 3), so reversibility of the couple is not compromised by any coupled chemical reactions.

The pH dependence of the Uf_o/Uf_r redox potential was investigated in the range $3 < pH < 7$, where the enzyme is known to be stable and active (*13*). Such experiments provide information on coupled electron/proton-transfer reactions at the active site. For example, a linear variation of −59 mV/pH unit for a single electron transfer is indicative of a single deprotonation accompanying oxidation (and protonation accompanying reduction). The redox potentials were determined by square wave voltammetry, which agreed with the averaged cyclic voltammetry peak potentials, and the data appear in Figure 4. Total electrochemical reversibility was maintained across the pH range studied. Above pH 5.5, the Uf_o/Uf_r redox potentials determined here coincide, within experimental uncertainty, with those reported by Wang et al. (*34*), although there is divergence below pH 5, where the potentials determined here approach a plateau whereas those determined by microcoulometry continue to rise linearly with decreasing pH.

The variation in redox potentials ($E(H^+)$) with pH observed here is consistent with an active site pK_a of ca. 5.2 for Uf_o according to eq 1 (*42*) for a single electron-transfer reaction coupled to proton transfer.

$$E(H^+) = E^o + \frac{RT}{F}\ln\left(\frac{K_a(Uf_r) + [H^+]}{K_a(Uf_o) + [H^+]}\right) + \frac{RT}{F}\ln\left(\frac{K_a(Uf_o)}{K_a(Uf_r)}\right) \quad (1)$$

In this case, at acidic-neutral pH values, Uf_r is in its protonated form (i.e., $K_a(Uf_r) \ll [H^+]$); thus, $K_a(Uf_r)$ may

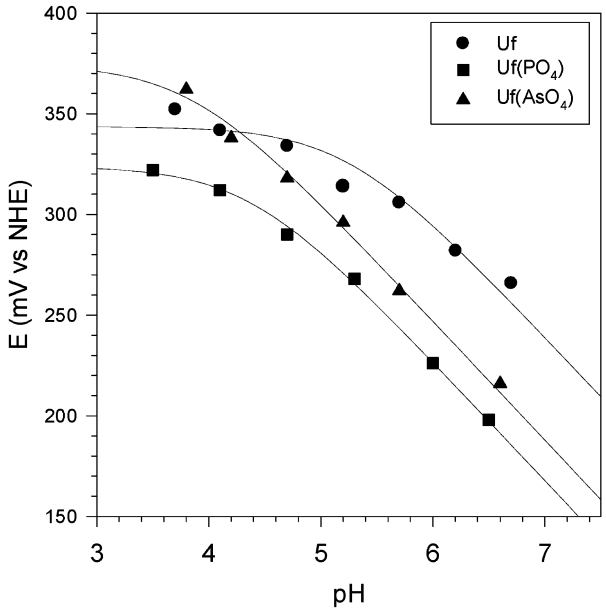

FIGURE 4: Redox potentials of Uf (●) and its phosphate (■) and arsenate (▲) complexes as a function of pH. The solid lines were calculated from eq 1 with p$K_a(Uf_o)$ = 5.2; p$K_a(Uf_o/PO_4)$ = 4.4, and p$K_a(Uf_o/AsO_4)$ = 3.8.

be neglected from second term of eq 1, and the first and third terms are pH independent. On the basis of crystallographic and spectroscopic data for PAPs, the site of deprotonation on Uf upon oxidation is most likely the terminal aqua ligand bonded to the redox active ferrous ion.

Similar cyclic voltammetry and square wave voltammetry experiments were performed for the phosphate and arsenate bound forms of Uf. Again, no change in the totally reversible cyclic voltammetry was found upon addition of either anion. These oxoanions are known (*23*) to be rather weak competitive inhibitors of Uf_r ($K_d \approx 1-25$ mM), so a large excess of each anion was employed to ensure saturation of both Uf_r and Uf_o during electrochemistry.

The pH-dependent redox potentials of the phosphate and arsenate complexes were fit to eq 1, and values of p$K_a(Uf_o/PO_4)$ = 4.4 and p$K_a(Uf_o/AsO_4)$ = 3.8 were determined. Displacement of the ferrous-bound terminal water-based ligand removes the group thought to be deprotonated (pK_a 5.2) upon oxidation of Uf_r. By elimination, it appears that the pK_a values determined for Uf_o/PO_4 and Uf_o/AsO_4 correspond to ionizations of the protonated coordinated anions themselves. The acid dissociation constants for dihydrogenphosphate (pK_a 7.2) and dihydrogenarsenate (pK_a 7.0) are upper bounds for the corresponding values of the coordinated anions since inductive effects of the metal ions must raise their acidities. Therefore, we propose that the observed Uf_o/XO_4 pK_a values correspond to deprotonation of the coordinated $H_2XO_4^-$ anions upon oxidation of Uf_r/PO_4. It is not known whether phosphate binds to Uf_r in a monodentate or bridging bidentate mode. EPR and kinetic studies by Merkx et al. suggest (*43*) that phosphate acts as a bridging ligand in Uf_r/PO_4 below pH 6.5 (the range we have investigated) but that monodentate coordination occurs at higher pH. A bridging bidentate coordination mode in Uf_r/PO_4 has also been suggested from mechanistic studies with Uf_r and other divalent metal derivatives. (*28*)

Table 1: Electrochemical Data and Derived Anion Complex Dissociation Constants

	pH	Δ^E (mV)	$K_d(Uf_r/XO_4)$ (mM)[a]	$K_d(Uf_o/XO_4)$ (mM)[b]
phosphate	3.0	−20	0.8	0.4
	4.0	−27	3.8	1.3
	4.5	−37	6.2	1.5
	4.9	−49	14	2.1
	5.5	−62	22	2.0
	6.0	−68	25	1.8
arsenate	4.9	−24	1.3	0.5
	6.0	−48	2.0	0.3

[a] Data from ref *23*. [b] From this work, calculated using eq 3.

As mentioned previously, Uf_r is inhibited by a variety of tetraoxo anions such as phosphate and arsenate, and it has been known for some time (*23*, *44*) that phosphate binding potentiates the aerobic oxidation of Uf_r, which is normally air stable. These observations suggested that the Uf redox potential is shifted cathodically in the presence of phosphate. The results of Wang et al. (*34*) and the work presented herein confirm this. The corollary of this in electrochemical terms is that the Uf redox potential in the presence of an oxoanion inhibitor (XO_4) will be cathodically shifted if binding to the oxidized form is stronger than that to the reduced form according to eq 2 (*42*), a variant on eq 1 involving complexation equilibria rather than protonation equilibria.

$$E(XO_4) = E^o + \frac{RT}{F}\ln\left(\frac{K_d(Uf_r/XO_4) + [XO_4]}{K_d(Uf_o/XO_4) + [XO_4]}\right) + \frac{RT}{F}\ln\left(\frac{K_d(Uf_o/XO_4)}{K_d(Uf_r/XO_4)}\right) \quad (2)$$

In the presence of saturating concentrations of the anion (i.e., where both Uf_o and Uf_r have an oxoanion bound at the active site), the second term of eq 2 vanishes and we arrive at eq 3, which gives the ratio of complex dissociation constants from the difference (ΔE) between the redox potentials of the complexed and free enzymes.

$$\Delta E = E(Uf/XO_{4,sat}) - E^o = \frac{RT}{F}\ln\left(\frac{K_d(Uf_o/XO_4)}{K_d(Uf_r/XO_4)}\right) \quad (3)$$

It should be noted that the phosphate and arsenate complex dissociation constants are pH dependent (*23*), and so too will be ΔE. The relevant literature data and experimental results are assembled in Table 1. Using eq 1 and the determined pK_a values for Uf_o, $Uf_o(PO_4)$, and $Uf_o(AsO_4)$, we calculated ΔE values to correspond with pH values at which the Uf_r complex dissociation constants with phosphate and arsenate have been reported and then used eq 3 to calculate $K_d(Uf_o(XO_4))$ at the corresponding pH value. It can be seen that ΔE increases as the pH is raised, but interestingly, the $K_d(Uf_o(XO_4))$ values are essentially pH independent. Although no dissociation constant data for arsenate binding to Uf_r at low pH are available, our results indicate that below pH 4.5 arsenate binds more tightly to Uf_r than to Uf_o ($\Delta E > 0$) in contrast to phosphate, which is more strongly bound to Uf_o at all pH values investigated. This feature has not been noted previously and reflects a subtle but significant difference between the two anions in their interactions with the active site.

The results presented in Table 1 are now compared with those of Wang et al. (*34*), who used mediated microcoulometry to determine ΔE values and hence dissociation constants for Uf_o (eq 3) with phosphate and arsenate at pH 5.0 and 6.0. The microcoulometry study reported ΔE values (approximately −170 mV for phosphate and approximately −90 mV for arsenate), about twice as large as those found here from cyclic voltammetry. Although we were able to study the complexation behavior over a much wider pH range and also at several different pH values, our calculated binding constants are 1 to 2 orders of magnitude weaker than those determined by microcoulometry. In the absence of $K_d(Uf_o/XO_4)$ values determined by other methods, we cannot offer an explanation for this variance. If the values of Wang et al. represent the true equilibrium constants in solution, then there may be a specific effect associated with immobilization of the enzyme within a surfactant film that weakens oxoanion binding in its oxidized form. Why this effect should lead to smaller differential inhibitor binding, and not to an across-the-board influence felt equally by Uf_r and Uf_o, is not clear, and further speculation seems unwarranted until more thermodynamic data become available on the binding of oxoanions by Uf_o.

CONCLUSIONS

For the first time, we have successfully investigated the direct electrochemistry of a purple acid phosphatase. Indeed, reports of the direct electrochemistry of any other dinuclear iron containing protein have been sparse, with the soluble methane monooxygenase being the sole example (*45*, *46*). The advantages of the direct electrochemical techniques described herein over mediated potentiometric or microcoulometric titrations are many (*35*). Rapid data acquisition using cyclic voltammetry is possible enabling the study of a wide range of pH values to be undertaken with the same aliquot of protein solution within a short time interval (~60 min). Second, the amount of protein used in this work for a full pH profile (~1 nmol), although large by comparison with our previous electrochemical studies using DDAB surfactant films, is much less than that needed for microcoulometry (~20 nmol for each pH determination). Also, voltammetrically determined redox potentials are inherently more precise, as they correspond with current maxima derived from several thousand data (current−voltage) points, whereas potentiometrically and coulometrically determined redox potentials are derived from Nernstian fits to a dozen or so experimental points. Cyclic voltammetry also enables the study of time-dependent coupled chemical reactions that may affect the reversibility of a particular electron-transfer reaction. In this study, we found no pH or oxoanion effect on the reversibility of the Uf redox couple, with totally reversible responses being observed in all cases. This work represents the first voltammetric investigation of an interesting class of enzymes. Opportunities now exist to probe the effect of other inhibitors on the redox properties of these proteins, and hopefully this work and future studies will lead to a greater understanding of the role of these interesting metalloenzymes and their mechanism.

REFERENCES

1. Klabunde, T., and Krebs, B. (1997) The dimetal center in purple acid phosphatases, *Struct. Bonding 89*, 177−198.
2. Twitchett, M. B., and Sykes, A. G. (1999) Structure, properties, and reactivity of the Fe(II)Fe(III) and Zn(II)Fe(III) purple acid phosphatases, *Eur. J. Inorg. Chem.*, 2105−2115.
3. Solomon, E. I., Brunold, T. C., Davis, M. I., Kemsley, J. N., Lee, S.-K., Lehnert, N., Neese, F., Skulan, A. J., Yang, Y.-S., and Zhou, J. (2000) Geometric and Electronic Structure/Function Correlations in Non-Heme Iron Enzymes, *Chem. Rev. 100*, 235−349.
4. Beck, J. L., de Jersey, J., Zerner, B., Hendrich, M. P., and Debrunner, P. G. (1988) Properties of the Fe(II) −Fe(III) derivative of red kidney bean purple phosphatase. Evidence for a binuclear zinc−iron center in the native enzyme, *J. Am. Chem. Soc. 110*, 3317−3318.
5. Schenk, G., Ge, Y., Carrington, L. E., Wynne, C. J., Searle, I. R., Carroll, B. J., Hamilton, S., and de Jersey, J. (1999) Binuclear Metal Centers in Plant Purple Acid Phosphatases: Fe−Mn in Sweet Potato and Fe−Zn in Soybean, *Arch. Biochem. Biophys. 370*, 183−189.
6. Schenk, G., Boutchard, C. L., Carrington, L. E., Noble, C. J., Moubaraki, B., Murray, K. S., de Jersey, J., Hanson, G. R., and Hamilton, S. (2001) A purple acid phosphatase from sweet potato contains an antiferromagnetically coupled binuclear Fe−Mn center, *J. Biol. Chem. 276*, 19084−19088.
7. Bozzo, G. G., Raghothama, K. G., and Plaxton, W. C. (2004) Structural and kinetic properties of a novel purple acid phosphatase from phosphate-starved tomato (*Lycopersicon esculentum*) cell cultures, *Biochem. J. 377*, 419−428.
8. Campbell, H. D., Dionysius, D. A., Keough, D. T., Wilson, B. E., de Jersey, J., and Zerner, B. (1978) Iron-containing acid phosphatases: comparison of the enzymes from beef spleen and pig allantoic fluid, *Biochem. Biophys. Res. Commun. 82*, 615−620.
9. Averill, B. A., Davis, J. C., Burman, S., Zirino, T., Sanders-Loehr, J., Loehr, T. M., Sage, J. T., and Debrunner, P. G. (1987) Spectroscopic and magnetic studies of the purple acid phosphatase from bovine spleen, *J. Am. Chem. Soc. 109*, 3760−3767.
10. Schenk, G., Korsinczky, M. L. J., Hume, D. A., Hamilton, S., and de Jersey, J. (2000) Purple acid phosphatases from bacteria: similarities to mammalian and plant enzymes, *Gene 255*, 419−424.
11. Oddie, G. W., Schenk, G., Angel, N. Z., Walsh, N., Guddat, L. W., De Jersey, J., Cassady, A. I., Hamilton, S. E., and Hume, D. A. (2000) Structure, function, and regulation of tartrate-resistant acid phosphatase, *Bone 27*, 575−584.
12. Marshall, K., Nash, K., Haussman, G., Cassady, I., Hume, D., de Jersey, J., and Hamilton, S. (1997) Recombinant human and mouse purple acid phosphatases: expression and characterization, *Arch. Biochem. Biophys. 345*, 230−236.
13. Valizadeh, M., Schenk, G., Nash, K., Oddie, G. W., Guddat, L. W., Hume, D. A., de Jersey, J., Burke, T. R., and Hamilton, S. (2004) Phosphotyrosyl peptides and analogues as substrates and inhibitors of purple acid phosphatases, *Arch. Biochem. Biophys. 424*, 154−162.
14. Guddat, L. W., McAlpine, A. S., Hume, D., Hamilton, S., de Jersey, J., and Martin, J. L. (1999) Crystal structure of mammalian purple acid phosphatase, *Structure 7*, 757−767.
15. Uppenberg, J., Lindqvist, F., Svensson, C., Ek-Rylander, B., and Andersson, G. (1999) Crystal structure of a mammalian purple acid phosphatase, *J. Mol. Biol. 290*, 201−211.
16. Straeter, N., Klabunde, T., Tucker, P., Witzel, H., and Krebs, B. (1995) Crystal structure of a purple acid phosphatase containing a dinuclear Fe(III)−Zn(II) active site, *Science 268*, 1489−1492.
17. Klabunde, T., Straeter, N., Froehlich, R., Witzel, H., and Krebs, B. (1996) Mechanism of Fe(III)−Zn(II) purple acid phosphatase based on crystal structures, *J. Mol. Biol. 259*, 737−748.
18. True, A. E., Scarrow, R. C., Randall, C. R., Holz, R. C., and Que, L., Jr. (1993) EXAFS studies of uteroferrin and its anion complexes, *J. Am. Chem. Soc. 115*, 4246−4255.
19. Wang, X., Randall, C. R., and Que, L., Jr. (1996) X-ray Absorption Spectroscopic Studies of the FeZn Derivative of Uteroferrin, *Biochemistry 35*, 13946−13954.
20. Wang, X., and Que, L., Jr. (1998) Extended X-ray Absorption Fine Structure Studies of the Anion Complexes of Fe−Zn Uteroferrin, *Biochemistry 37*, 7813−7821.
21. Smoukov, S. K., Quaroni, L., Wang, X., Doan, P. E., Hoffman, B. M., and Que, L., Jr. (2002) Electron−Nuclear Double Resonance Spectroscopic Evidence for a Hydroxo Bridge Nucleophile Involved in Catalysis by a Dinuclear Hydrolase, *J. Am. Chem. Soc. 124*, 2595−2603.
22. Lauffer, R. B., Antanaitis, B. C., Aisen, P., and Que, L., Jr. (1983) Proton NMR studies of porcine uteroferrin. Magnetic interactions and active site structure, *J. Biol. Chem. 258*, 14212−14218.
23. Pyrz, J. W., Sage, J. T., Debrunner, P. G., and Que, L., Jr. (1986) The interaction of phosphate with uteroferrin. Characterization of a reduced uteroferrin−phosphate complex, *J. Biol. Chem. 261*, 11015−11020.
24. David, S. S., and Que, L., Jr. (1990) Anion binding to uteroferrin. Evidence for phosphate coordination to the iron(III) ion of the dinuclear active site and interaction with the hydroxo bridge, *J. Am. Chem. Soc. 112*, 6455−6463.
25. Scarrow, R. C., Pyrz, J. W., and Que, L., Jr. (1990) NMR studies of the dinuclear iron site in reduced uteroferrin and its oxoanion complexes, *J. Am. Chem. Soc. 112*, 657−665.
26. Aquino, M. A. S., and Sykes, A. G. (1994) Redox reactivity of the binuclear iron active site of porcine purple acid phosphatase (uteroferrin), *J. Chem. Soc., Dalton Trans.* 683−687.
27. Wynne, C. J., Hamilton, S. E., Dionysius, D. A., Beck, J. L., and de Jersey, J. (1995) Studies on the catalytic mechanism of pig purple acid phosphatase, *Arch. Biochem. Biophys. 319*, 133−141.
28. Twitchett, M. B., Schenk, G., Aquino, M. A. S., Yiu, D. T. Y., Lau, T.-C., and Sykes, A. G. (2002) Reactivity of M^{II} Metal-Substituted Derivatives of Pig Purple Acid Phosphatase (Uteroferrin) with Phosphate, *Inorg. Chem. 41*, 5787−5794.
29. Debrunner, P. G., Hendrich, M. P., De Jersey, J., Keough, D. T., Sage, J. T., and Zerner, B. (1983) Mössbauer and EPR study of the binuclear iron center in purple acid phosphatase, *Biochim. Biophys. Acta 745*, 103−106.
30. Rodriguez, J. H., Ok, H. N., Xia, Y. M., Debrunner, P. G., Hinrichs, B. E., Meyer, T., and Packard, N. H. (1996) Mössbauer Spectroscopy of the Spin-Coupled Fe^{3+}−Fe^{2+} Center of Reduced Uteroferrin, *J. Phys. Chem. 100*, 6849−6862.
31. Keough, D. T., Dionysius, D. A., de Jersey, J., and Zerner, B. (1980) Iron-containing acid phosphatases: characterization of the metal-ion binding site of the enzyme from pig allantoic fluid, *Biochem. Biophys. Res. Commun. 94*, 600−605.
32. Holz, R. C., Que, L., Jr., and Ming, L. J. (1992) NOESY studies on the Fe(III)Co(II) active site of the purple acid phosphatase uteroferrin, *J. Am. Chem. Soc. 114*, 4434−4436.
33. Merkx, M., and Averill, B. A. (1999) Probing the role of the trivalent metal in phosphate ester hydrolysis: preparation and characterization of purple acid phosphatases containing $Al^{III}Zn^{II}$ and $In^{III}Zn^{II}$ active sites, including the first example of an active aluminum enzyme, *J. Am. Chem. Soc. 121*, 6683−6689.
34. Wang, D. L., Holz, R. C., David, S. S., Que, L., Jr., and Stankovich, M. T. (1991) Electrochemical properties of the diiron core of uteroferrin and its anion complexes, *Biochemistry 30*, 8187−8194.
35. Armstrong, F. A., and Wilson, G. S. (2000) Recent developments in faradaic bioelectrochemistry, *Electrochim. Acta 45*, 2623−2645.
36. Aquino, M. A. S., Lim, J. S., and Sykes, G. (1992) Mechanism of the reaction of phosphate with purple acid phosphatase, *J. Chem. Soc., Dalton Trans.* 2135−2136.
37. Aguey-Zinsou, K. F., Bernhardt, P. V., and Leimkühler, S. (2003) Protein Film Voltammetry of *Rhodobacter capsulatus* Xanthine Dehydrogenase, *J. Am. Chem. Soc. 125*, 15352−15358.
38. Heering, H. A. (2001) UTILS, Utilities for Data Analysis, University of Delft, The Netherlands.
39. Bard, A. J., and Faulkner, L. R. (2001) Electrochemical Methods: Fundamentals and Applications, 2nd ed., Wiley, New York.
40. Aguey-Zinsou, K.-F., Bernhardt, P. V., De Voss, J. J., and Slessor, K. E. (2003) Electrochemistry of $P450_{cin}$: new insights into P450 electron transfer, *Chem. Commun.*, 418−419.
41. Aguey-Zinsou, K.-F., Bernhardt, P. V., McEwan, A. G., and Ridge, J. P. (2002) The first nonturnover voltammetric response from a molybdenum enzyme: direct electrochemistry of dimethyl sul-

foxide reductase from *Rhodobacter capsulatus*, *J. Biol. Inorg. Chem. 7*, 879−883.

42. Clark, W. M. (1960) The Oxidation−Reduction Potentials of Organic Systems, The Williams and Wilkins Company, Baltimore.
43. Merkx, M., Pinkse, M. W. H., and Averill, B. A. (1999) Evidence for Nonbridged Coordination of *p*-Nitrophenyl Phosphate to the Dinuclear Fe(III)−M(II) Center in Bovine Spleen Purple Acid Phosphatase during Enzymatic Turnover, *Biochemistry 38*, 9914−9925.
44. Keough, D. T., Beck, J. L., de Jersey, J., and Zerner, B. (1982) Iron-containing acid phosphatases: interaction of phosphate with the enzyme from pig allantoic fluid, *Biochem. Biophys. Res. Commun. 108*, 1643−1648.
45. Kazlauskaite, J., Hill, H. A. O., Wilkins, P. C., and Dalton, H. (1996) Direct electrochemistry of the hydroxylase of soluble methane monooxygenase from *Methylococcus capsulatus*, *Eur. J. Biochem. 241*, 552−556.
46. Astier, Y., Balendra, S., Hill, H. A. O., Smith, T. J., and Dalton, H. (2003) Cofactor-independent oxygenation reactions catalyzed by soluble methane monooxygenase at the surface of a modified gold electrode, *Eur. J. Biochem. 270*, 539−544.

BI0490338